Desalination and Water Treatment
www.deswater.com

doi: 10.1080/19443994.2013.873880

53 (2015) 3521–3530
March

Taylor & Francis
Taylor & Francis Group

Removal of heavy metals from aqueous solution by multiwalled carbon nanotubes: equilibrium, isotherms, and kinetics

M.R. Lasheen[a], Iman Y. El-Sherif[a], Dina Y. Sabry[b], S.T. El-Wakeel[a,*], M.F. El-Shahat[b]

[a]*Water Pollution Research Department, Environmental Research Division, National Research Centre, 33-El Buhouth Street, Dokki, Cairo 12311, Egypt*
Tel. + 202 33371211; Fax: + 202 33370931; email: shaimaa_tw@yahoo.com
[b]*Faculty of Science, Ain Shams University, Khalifa El-Maamon St, Abbasiya Sq, Cairo 11566, Egypt*

Received 16 October 2013; Accepted 25 November 2013

ABSTRACT

The adsorption of heavy metal ions (Cu^{2+}, Pb^{2+}, Cd^{2+}, Ni^{2+}, and Cr^{6+}) on as-produced and oxidized multiwalled carbon nanotubes (MWCNTs) was investigated as a function of contact time, pH, and dose used in batch technique. The results indicated that the adsorption capacity of metals onto oxidized MWCNTs was greater than that on as-produced MWCNTs. The adsorption on oxidized MWCNTs increased with pH and increased dose. The affinity order of the studied metals was found to be Pb^{2+}> Cu^{2+}> Cr^{6+}> Cd^{2+}> Ni^{2+}. The adsorption process achieved equilibrium within 2 h, and experimental data fitted well the pseudo-second-order model.

Keywords: Carbon nanotubes; Heavy metals; Adsorption

1. Introduction

Environmental pollution of heavy metals, such as cadmium, chromium, copper, lead, and nickel, has received considerable attention worldwide because of their toxicity on metabolism and intelligence. They can be readily adsorbed by marine animals and directly enter the human food chains, thus presenting a high health risk to consumers [1].

There are many conventional methods that are being used to remove heavy metal ions including reduction, precipitation, membrane filtration, ion exchange, and adsorption. Among these methods, a promising process for the removal of metal ions from water and wastewater is adsorption, because of its simplicity, convenience, and because the employed adsorbent can be regenerated by the suitable deception process. Several adsorbents have been studied for adsorption of metal ions, such as activated carbon [2,3], fly ash [4,5], peat [6], sewage sludge ash [7], zeolite [8], kaolinite [9], and resins [10].

In recent years, nanotechnology has introduced different types of nanomaterials to the water industry that can have promising outcomes. Carbon nanotubes (CNTs) are one of the new nanosorbents that have been discovered in 1991 by Iijima [11] and recently found to be able to remove a wide range of contaminants and heavy metals, such as Cr^{3+} [12], Pb^{2+} [13], Zn^{2+} [14], Cd^{2+} [15], Cu^{2+} [16], Cr^{6+} [17], and Ni^{2+} [18] from water. CNTs include single-walled CNTs (SWCNTs) and multiwalled CNTs (MWCNTs) depending on the amount of layers.

*Corresponding author.

Because of their structural properties with nanometer-order size and pseudo-graphite layers, MWCNTs have been expected to be applied for the electrochemical storage of hydrogen and a promising sorbent of heavy metal ions and radionuclides [19].

The objectives of the present study are (1) to investigate the adsorption capacity of as-produced and oxidized multiwalled carbon nanotubes (MWCNTs) for Cu^{2+}, Cd^{2+}, Pb^{2+}, Ni^{2+}, and Cr^{6+} metal ions, (2) to study the effects of contact time, initial pH, and dose on the adsorption, and (3) to investigate the adsorption isotherm and kinetics of metals' adsorption onto MWCNTs.

2. Materials and methods

2.1. Materials

MWCNTs were purchased from Sigma–Aldrich (Steinheim, Germany) with outer diameter of 7–15 nm, length of 0.5–10 μm, and density of ~2.1 g/mL at 25°C. The MWCNTs obtained were prepared by electric arc discharge method. As-produced MWCNTs were oxidized by dispersion into a flask containing concentrated nitric acid solution and refluxed at 140°C for 6 h. The suspension was washed with deionized water to remove excess oxidant. Then, the oxidized CNTs, denoted as "MWCNTs-ox", were dried at 100°C and stored for further studies. All the other agents used were of analytical grade.

2.2. Analytical methods

The phase structures of CNTs were characterized by powder X-ray diffraction (XRD, Bruker D8 advance instrument). The instrument was equipped with a copper anode generating (Cu-Kα) radiation ($\lambda = 1.5406$ Å). The size and morphology of the CNTs were elucidated by transmission electron microscopy (TEM) using JOEL JEM (1230) electron microscope instrument with resolving resolution of 0.2 nm.

The functional groups of CNTs were identified by Fourier transform infrared spectroscopy (FT-IR) analysis using FT-IR-6100 (JASCO-Japan) instrument via the KBr pressed disk method. Gas adsorption analyzer with Brunauer–Emmett–Teller method (Quantachrome NOVA Automated gas sorption systems-1.12) was used for the surface area determination, where N_2 gas was used as adsorbate at 77 K.

The concentration of metals in the solution was determined according to APHA [20] using atomic absorption spectrometer (Varian Spectra AAS 220) with graphite furnace accessory and equipped with deuterium arc background corrector.

2.3. Batch adsorption experiments

The adsorption behavior of as-produced MWCNT and MWCNT-ox for metal ions Cu^{2+}, Cd^{2+}, Pb^{2+}, Ni^{2+}, and Cr^{6+} was investigated by means of the batch experiments at room temperature (~25°C). Batch adsorption experiments were conducted using different doses of as-produced MWCNT and MWCNT-ox ranging from 0.1 to 4 g/L of solutions containing heavy metal ions of desired concentrations (20 mg/L) for each metal. The adsorption of metals was investigated in the pH range of 2–8. The solution pH was adjusted by 0.1 M NaOH and 0.1 M HNO_3. The bottles were shaken in a rotary shaker at 200 rpm at different contact times from 5 to 140 min.

The equilibrium adsorption capacity, q_e (mg/g), of the metal was calculated using the mass balance, according to Eq. (1):

$$q_e = (C_0 - C_e)V/m \tag{1}$$

where V is the sample volume (L), m is the mass of the adsorbents (g), C_0 is the initial metal concentration (mg/L), and C_e is the equilibrium concentration of the metal in the solution (mg/L).

2.4. Desorption of metal and reusability of CNTs

In this experiment, desorption of metals from metal-loaded nanoadsorbents was performed using 5 M HNO_3 solution. MWCNT-ox-loaded metals was exposed to 10 mL of 5 M HNO_3 and agitated at 200 rpm for 2 h. After the desorption, the nanoadsorbent was separated by filtration and metals' concentrations were measured. The recovery efficiency, r (%), of metals from the solid phase was calculated by Eq. (2) [21]:

$$r(\%) = \frac{C_{des}}{C_{ads}} \times 100 \tag{2}$$

where C_{des} and C_{ads} are the amount of metal released into the aqueous solution and the amount of metal adsorbed onto the nanoadsorbents (mg/L), respectively.

To test the reusability of the nanoadsorbent, 10 of 50 mg/L metals' solution was mixed with 20 mg of nanoadsorbents for 2 h and then desorbed by the addition of 10 mL of 5 M HNO_3 with stirring for 2 h. After each cycle of adsorption–desorption, the adsorbent was washed thoroughly with distilled water to neutrality, dried, and reconditioned for adsorption in the succeeding cycle.

3. Results and discussion

3.1. Characterization of MWCNTs

Fig. 1 displays the TEM images of as-produced MWCNTs and MWCNT-ox. As can be observed, MWCNT have very smooth surfaces and cylindrical shapes with an external diameter of 1–7 nm.

The XRD patterns of as-produced MWCNTs and MWCNT-ox are given in Fig. 2. The most intense peaks of MWCNTs-ox are at the (26) and (42.4) reflections, which can be attributed to the hexagonal graphite structures (002), (100). The surface area of MWCNT-ox is 279.8 m^2/g with total pore volume of 0.083 cm^3/g.

The FT-IR spectra charts for the CNTs are presented in Fig. 3. For both materials, the bands in the spectrum at 800–1,400 cm^{-1} can be attributed to the stretching vibrations of C–C and –C–H. The broad band at 3,200–3,600 cm^{-1} represents hydroxyl and carboxylic groups. The signature of C=O functional groups is evident at 1,650 cm^{-1} and OH functional groups appear at 3,500 cm^{-1}.

Oxygen-containing functional groups for as-produced MWCNT may come from the acid washing to remove the catalyst when being fabricated. After oxidative treatment with nitric acid the bands are much more pronounced.

3.2. Adsorption studies

3.2.1. Effect of contact time

The effect of contact time on the removal of metal ions (Cu^{2+}, Cd^{2+}, Pb^{2+}, Ni^{2+}, and Cr^{6+}) from aqueous solutions was investigated for both the as-produced and oxidized MWCNTs for 140 min. The initial metals' concentration was 20 mg/L with an adsorbent dose of 2 g/L and shaking speed of 200 rpm.

The sorption capacity of metal ions onto CNTs increased quickly with contact time and then slowly reached equilibrium in 120 min. As can be seen in Fig. 4(a) and (b), the adsorption capacities of metals onto MWCNT-ox are higher than those onto as-produced MWCNTs.

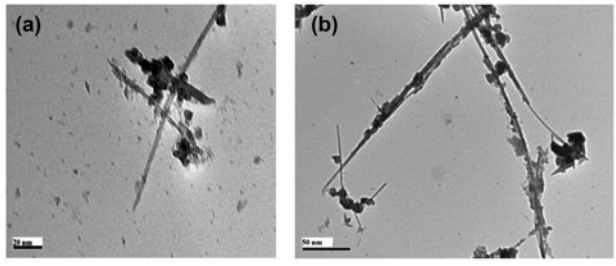

Fig. 1. TEM images of (a) as-produced MWCNT and (b) MWCNT-ox.

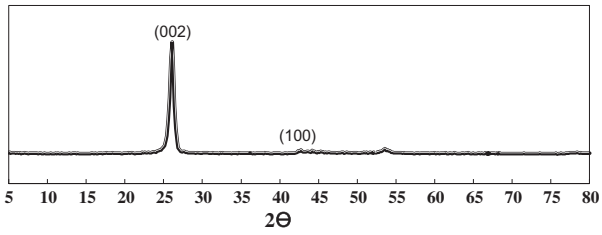

Fig. 2. XRD pattern of MWCNT-ox.

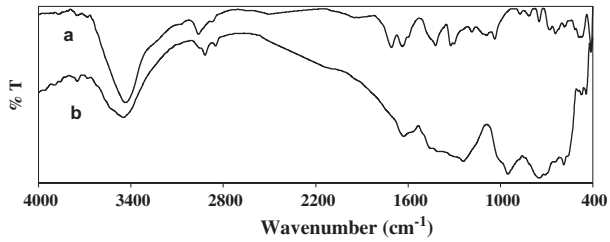

Fig. 3. FT-IR spectra of (a) as-produced MWCNT and (b) MWCNT-ox.

Li et al. [13] found that the sorption capacity of Pb^{2+} onto CNTs increased quickly with contact time and then slowly reached equilibrium in 50 min at an initial concentration (C_0) of 20 mg/L. Lu and Liu [22] reported that the Ni^{2+} sorption reached equilibrium in 60 and 120 min with C_0 of 10 and 60 mg/L, respectively. CNTs adsorb metals in the order $Pb^{2+} > Cu^{2+} > Cr^{6+} > Cd^{2+} > Ni^{2+}$. Results obtained by Lia [16] concluded that CNTs' adsorption showed affinity in the order of $Pb^{2+} > Cu^{2+} > Cd^{2+}$.

3.2.2. Effect of initial pH

The effect of initial pH on the adsorption uptake of metal ions (Cu^{2+}, Cd^{2+}, Pb^{2+}, Ni^{2+}, and Cr^{6+}) was investigated for both the as-produced and oxidized MWCNTs. The solution pH affects the surface charge of the adsorbent and the degree of ionization and speciation of the adsorbates.

Fig. 5(a) and (b) shows that as the pH increases, the adsorption increases for both MWCNTs due to the increase in the electrostatic attractive forces between OH^- and metal ions. The removal of Pb(II) increases very quickly from about 66 to 96% at pH 2–6.5.

At pH < 6, the predominant specie is Pb^{2+} and the removal of Pb^{2+} is mainly accomplished by sorption reaction. Therefore, the low Pb^{2+} sorption that takes

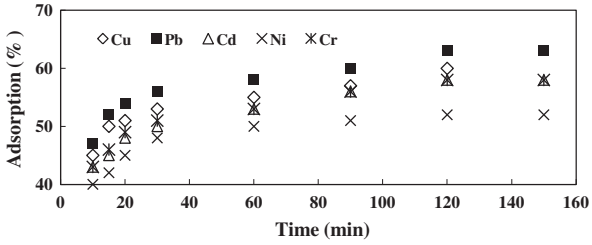

Fig. 4(a). Effect of contact time on metals adsorption by as-produced MWCNT (dose: 1 gm/L, initial metal concentration: 20 mg/L, and shaking rate: 200 rpm).

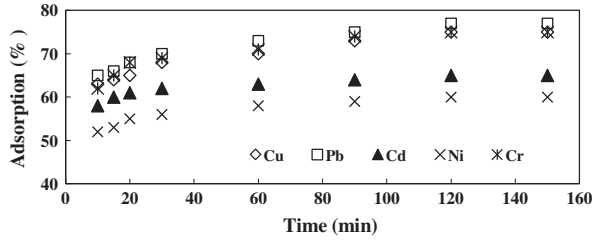

Fig. 4(b). Effect of contact time on metals adsorption by MWCNT-ox (dose: 1 gm/L, initial metal concentration: 20 mg/L, and shaking rate: 200 rpm).

place at low pH can be attributed partly to the competition between H^+ and Pb^{2+} ions on the surface sites [23].

Cu^{2+} removal increased to 98% for oxidized MWCNTs at pH 4. Overall, the dominant form of Cu (II) at pH 2.0 is Cu^{2+}, and with an increase in pH from 2.0 to 4.0 other species, including $Cu_2(OH)_2^{2+}$, $Cu(OH)^+$, $Cu_2(OH)^{3+}$, and $Cu_3(OH)_4^{2+}$, are formed. The adsorption experiments were not conducted at pHs above for Cu and above 7 for Pb because of Pb $(OH)_2$ and $CuOH)_2$ precipitation [23].

The removal efficiencies of $Cd^{2+}$and Ni^{2+} were gradually increased to 96 and 95%, respectively, with the pH increasing from 2 to 7 and 7.5.

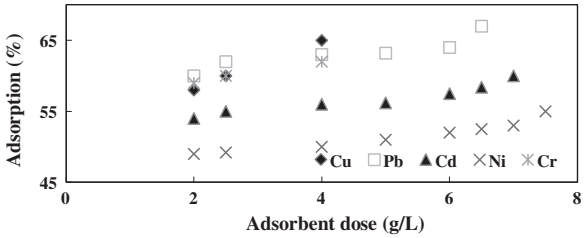

Fig. 5(a). Effect of pH on metals adsorption by as-produced MWCNT (contact time: 120 min, initial metal concentration: 20 mg/L, and shaking rate: 200 rpm).

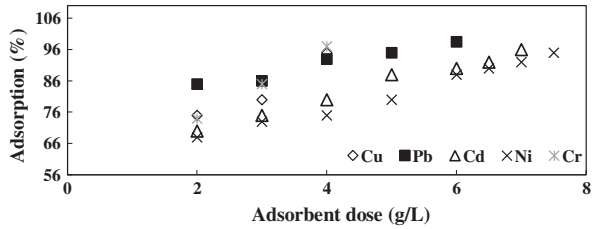

Fig. 5(b). Effect of pH on metals adsorption by MWCNT-ox (contact time: 120 min, initial metal concentration: 20 mg/L, pH: 5.5, and shaking rate: 200 rpm).

The dominant form of Ni is Ni^{2+}, and at pH 4.0 the species $Ni(OH)^-$ is formed. At pH above 7.5, adsorption experiments were not conducted for nickel as the precipitation of nickel hydroxide was observed. At pH values below 3, Ni^{2+} uptake was very weak due to the competition between Ni^{2+} and H^+ in the solution. Li et al. [15] showed that the adsorption of $Cd^{2+}$is higher in alkaline range. However, in this region a precipitate of $Cd(OH)_2$ is formed. They concluded that Cd^{2+} adsorption capacities of CNTs oxidized with HNO_3 reach 8.0 mg/g at pH value of 6.0, while they are only 2.0 mg/g for the as-grown CNTs.

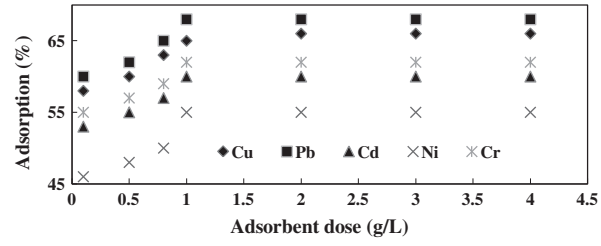

Fig. 6(a). Effect of adsorbent dose on metals adsorption by as-produced MWCNT (contact time: 120 min, initial metal concentration: 20 mg/L, pH: 5.5, and shaking rate: 200 rpm).

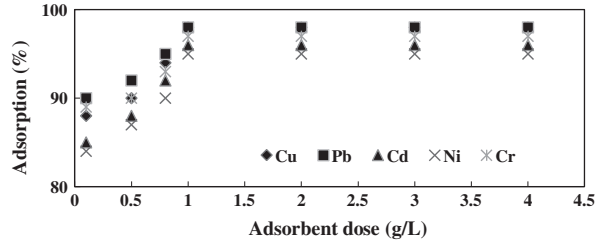

Fig. 6(b). Effect of adsorbent dose on metals adsorption by MWCNT-ox (contact time: 120 min, initial metal concentration: 20 mg/L, pH: 5.5, and shaking rate: 200 rpm).

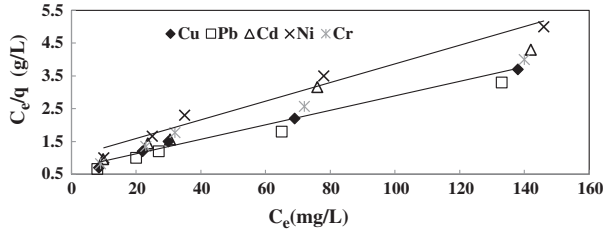

Fig. 7(a). The Langmuir isotherm plot for metals adsorption by as-produced MWCNT (pH: 5.5, contact time: 120 min, shaking rate: 200 rpm, and dose: 1 g/L).

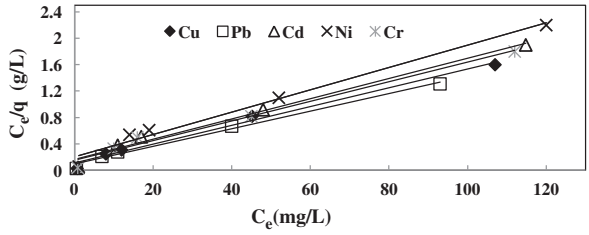

Fig. 7(b). The Langmuir isotherm plot for metals' adsorption by MWCNT-ox (pH: 5.5, contact time: 120 min, shaking rate: 200 rpm, and amount of adsorbent: 1 g/L).

Cadmium ions have a higher adsorption affinity to the nanoadsorbents than the ions of nickel. This affinity is related to a number of factors, such as molecular mass, ion charges, ionic radius, hydrated ionic radius, and hydration energy of the metals.

3.2.3. The effect of adsorbent dose

As the adsorbent dosage increases, the adsorption sites available for metals are also increased, and consequently better adsorption takes place. The adsorbent doses were varied from 0.1 to 4 g/L while all the other variables, such as contact time and temperature, were kept constant.

The results in Fig. 6(a) and (b) reveal that the removal of heavy metals increased with increasing MWCNTs' dose. The adsorption of all studied metals reaches equilibrium using 1 g/L of adsorbents.

3.3. Adsorption isotherms

The Langmuir, Freundlich, and Dubinin–Kaganer–Radushkevich are the most common isotherm models that describe the distribution of a metal ion between a solid and liquid phase.

Table 1
Freundlich, Langmuir and DKR isothermal adsorption equation parameters for the adsorption of Pb^{2+}, Cu^{2+}, Cr^{6+}, Cd^{2+} and Ni^{2} by as produced and oxidized MWCNT at room temperature (absorbent dose: 1 g/L, pH value: 5.5, metals concentration: 20–200 mg/L, contact time: 120 min, and agitation speed: 200 rpm)

	As produced MWCNT					Oxidized MWCNT				
	Pb^{2+}	Cu^{2+}	Cr^{6+}	Cd^{2+}	Ni^{2+}	Pb^{2+}	Cu^{2+}	Cr^{6+}	Cd^{2+}	Ni^{2+}
Freundlich isotherm parameters										
$1/n$	0.42	0.43	0.44	0.45	0.39	0.31	0.25	0.24	0.25	0.25
k_F (mg/g)	5.4	4.6	4.1	4	3.9	21.7	20.4	19	18	16.5
R^2	0.97	0.98	0.98	0.99	0.97	0.98	0.99	0.97	0.97	0.97
Langmuir isotherm parameters										
q_{max} (mg/g)	48	45	43	39	35	75	70.4	67	66	59.2
b (L/mg)	0.04	0.03	0.02	0.03	0.02	0.13	0.1	0.09	0.09	0.08
R^2	0.97	0.98	0.98	0.98	0.97	0.98	0.99	0.98	0.97	0.97
DKR isotherm parameters										
q_{max} (mol/g)	8.2×10^{-4}	5.4×10^{-4}	1.6×10^{-3}	1.2×10^{-3}	1.4×10^{-4}	7.8×10^{-4}	1.8×10^{-3}	2.2×10^{-3}	1.1×10^{-3}	3.1×10^{-3}
β (mol^2/J^2)	-0.360×10^{-8}	-0.46×10^{-8}	-6.39×10^{-8}	-0.36×10^{-8}	-0.5×10^{-8}	-0.22×10^{-8}	0.231×10^{-8}	0.24×10^{-8}	-0.26×10^{-8}	-0.34×10^{-8}
E (kJ/mol)	10.9	10.3	10.2	10	9.9	14.9	14.7	14.2	13.8	12
R^2	0.98	0.98	0.96	0.96	0.96	0.96	0.96	0.96	0.97	0.96

The Langmuir isotherm [24] assumes monolayer coverage of the adsorption surface and no subsequent interaction among adsorbed molecules. Therefore, the adsorption saturates, and no further adsorption can occur. The expression for the Langmuir isotherm is listed in Eq. (3):

$$\frac{C_e}{q_e} = \frac{1}{bq_{\max}} + \frac{C_e}{q_{\max}} \tag{3}$$

where q is the amount of metal ions sorbed per unit mass (mg/g), $q_{\max}$ is maximum adsorption capacity at complete monolayer coverage (mg/g), and b is a Langmuir constant that relates to the heat of adsorption (L/mg). The values of $q_{\max}$ and b were determined by plotting C_e/q_e vs. C_e.

Fig. 7(a) and (b) shows the adsorption data of metal ions on both the as-produced and oxidized MWCNTs. Results, as listed in Table 1, were fitted to the Langmuir equation.

The values of $q_{\max}$ obtained from Langmuir model for metal ions adsorption on MWCNTs-ox are higher than that from as-produced MWCNTs.

The Freundlich adsorption isotherm [25] suggests that the adsorption phenomenon occurred on heterogeneous surfaces. The isotherm assumes that the surface sites of the adsorbent have different binding energies. Eq. (4) describes Freundlich adsorption isotherm:

$$q_e = k_F C_e^{1/n} \tag{4}$$

Eq. (4) can be expressed in linear form by Eq. (5):

$$\log q_e = \log k_F + \frac{1}{n}\log C_e \tag{5}$$

where q_e is the equilibrium adsorption capacity, (mg/g), C_e is the equilibrium concentration of metals in the solution (mg/L), k_F represents the adsorption capacity when metal ion equilibrium concentration equals to1 (mg/g), and n is the degree of dependence of adsorption with equilibrium concentration and related to the sorption intensity of the adsorbent.

The Freundlich parameters, k_F and $1/n$, can be determined by plotting ln q_e vs. ln C_e (Fig. 8(a) and 8(b)).

The values of Freundlich constants, k_F and $1/n$, obtained are shown in Table 1. The high R^2 values obtained are shown in the table.

The values of $1/n$ were observed to be less than unity for all the adsorbents as shown in Table 1 indicating favorable adsorption [26]. The value of k_F calculated from the Freundlich model is large, which indicates that MWCNT-ox has a high adsorption affinity towards metals' ions.

These results suggest that both Langmuir and Freundlich isotherms show a good fit to the experimental data with well-matching correlation coefficients so that both monolayer sorption and heterogeneous distribution of active sites on the surface of the adsorbent occurs. Table 2 compares the adsorption capacity of some heavy metals on CNTs and other adsorbents in the literature.

The D–R isotherm model is valid at low concentration ranges and can be used to describe adsorption on both homogeneous and heterogeneous surfaces. The general expression of the D–R [30] isotherm can be described by Eq. (6):

$$\ln_q = \ln q_{\max} - \beta\varepsilon^2 \tag{6}$$

where β is the activity coefficient related to mean sorption energy (mol^2/kJ^2) and ε is the Polanyi potential, which can be calculated from Eq. (7):

$$\varepsilon = RT\ln\left(1 + \frac{1}{C_e}\right) \tag{7}$$

where R is the ideal gas constant (8.3145 J/mol K) and T is the absolute temperature (K).

The slope of the plot of ln q vs. ε^2 gives β (mol^2/J^2) and the intercept yields the maximum sorption capacity, $q_{\max}$ (mol /g).

Table 2
The adsorption capacity of some heavy metal ions on CNTs and other adsorbents

Adsorbent	Adsorption capacity (mg/g)	Metal	References
As-grown CNTs	4.83	Cu^{2+}	[27]
H2SO4-CNTs	14.37		
CNTs	97.08	Pb^{2+}	[16]
	28.49	Cu^{2+}	
	10.86	Cd^{2+}	
Kaolinite	10.79	Cu^{2+}, (25 ℃)	[28]
Zeolite	14.72	Cu^{2+} (pH=5, 30 ℃)	[29]
Fly ash	8.1	Cu^{2+}	[4]

E is defined as the free energy change (kJ/mol), which requires transferring 1 mol of ions from solution to the solid surfaces. The relation is listed in Eq. (8):

$$E = \frac{1}{\sqrt{-2\beta}} \tag{8}$$

The plot of ln q_e against ε^2 for metals adsorption MWCNTs is shown in Fig. 9(a) and (b), and DKR parameters are listed in Table 1.

The magnitude of E is useful for estimating the mechanism of the adsorption reaction. Adsorption is dominated by chemical ion exchange if E is in the range of 8–16 kJ/mol, whereas physical forces may affect the adsorption in the case of $E < 8$ kJ/mol [31]. The E values obtained from Eq. (9) are 14.9, 14.7, 14.2, 13.8, and 12 kJ/mol for Pb^{2+}, Cu^{2+}, Gr^{6+}, Cd^{2+}, and Ni $^{2+}$, respectively, for adsorption on MWCNT-ox and decreased to 10.9, 10.3, 10.2, 10, and 9.9 kJ/mol for adsorption on as-produced MWCNT. Values are in the adsorption energy range of chemical ion-exchange reactions. This suggests that metals' adsorption onto MWCNTs is attributed to chemical adsorption rather than physical adsorption.

3.4. Adsorption kinetics

Adsorption kinetics, demonstrating the solute uptake rate, is one of the most important characters which represent the adsorption efficiency of the MWCNTs, and therefore determines their potential applications.

Adsorption kinetics samples were prepared by adding 10 mg of as-produced and oxidized MWCNTs into 5 mL solution at the effective pH value for each metal (20 mg/L). 120 min is enough to achieve the adsorption equilibrium under our experimental conditions.

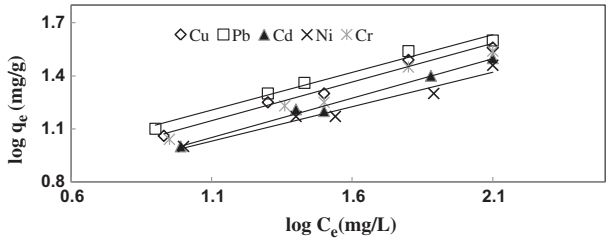

Fig. 8(a). The Freundlich isotherm plot for metals adsorption by as-produced MWCNT (pH: 5.5, contact time:120 min, shaking rate: 200 rpm, and dose: 1 g/L).

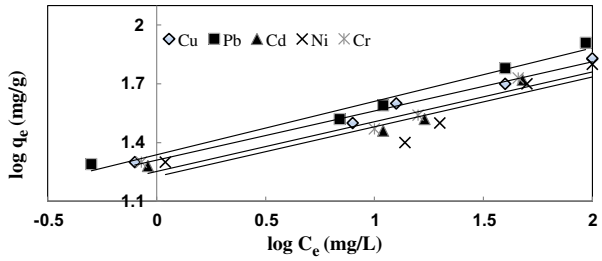

Fig. 8(b). The Freundlich isotherm plot for metals adsorption by MWCNT-ox (pH: 5.5, contact time: 120 min, shaking rate: 200 rpm, and amount of adsorbent: 1 g/L).

3.4.1. Pseud-first-order kinetics

The pseudo-first-order equation (Lagergren's equation) describes adsorption in solid–liquid systems based on the sorption capacity of solids.

The linear form of pseudo-first-order model can be expressed by Eq. (9) as [32]:

$$\log(q_e - q_t) = \log q_e - \frac{k_1 t}{2.303} \tag{9}$$

where q_e and q_t are the amounts of adsorbed metals on the adsorbent at equilibrium and at time t, respectively (mg/g), and k_1 is the first-order adsorption rate constant (min^{-1}).

The linearized forms of the pseudo-first-order model for the sorption of metals ions onto as-produced MWCNT and MWCNT-ox are given in Fig. 10(a) and (b). The calculated results of the first-order rate equation are given in Table 3. The q_e value acquired by this method contrasted with the experimental value. So, the reaction cannot be classified as first order.

3.4.2. Pseudo-second-order kinetics

Second-order kinetic equation was applied to find a more reliable description of the kinetics. The pseudo-second-order kinetics can be represented by the following linear Eq. (10) [33]:

$$\frac{t}{q_t} = \frac{1}{K_2 q_e^2} + \frac{1}{q_e} t \tag{10}$$

where k_2 is the pseudo-second-order rate constant of adsorption (g/mg min).

Linear plot of t/q_t vs. t is achieved according to Eq. (10) (Fig. 11(a) and (b)). The k and q_e values calculated from the slope and intercept of the plot are summarized in Table 3.

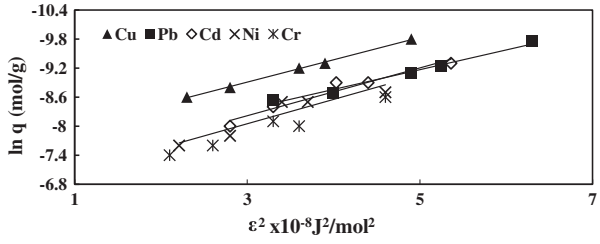

Fig. 9(a). The DKR isotherm plot for metals adsorption by as-produced MWCNT (pH: 5.5, contact time: 120 min, shaking rate: 200 rpm, and amount of adsorbent: 1 g/L).

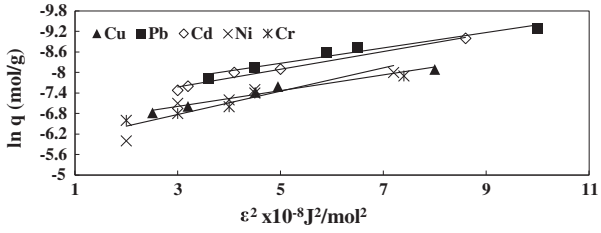

Fig. 9(b). The DKR isotherm plot for metals adsorption by MWCNT-ox (pH: 5.5, contact time: 120 min, shaking rate: 200 rpm, and amount of adsorbent: 1 g/L).

The calculated q_e values agreed very well with the experimental data. Since the correlation coefficients of the pseudo-second-order equation for the linear plots are very close to one, the pseudo-second-order kinetics was a pathway to reach the equilibrium and the rate-limiting step in adsorption is chemisorption.

3.4.3. Elovich kinetic model

The Elovich kinetic model [34] is based on chemisorption phenomena and is expressed by Eq. (11):

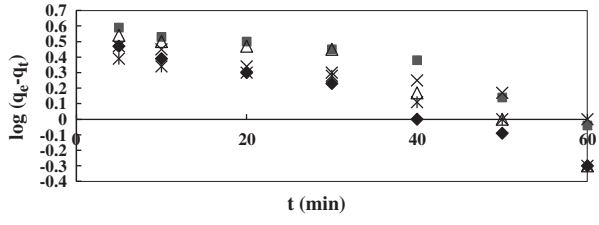

Fig. 10(a). Pseudo-first-order sorption kinetics of metals onto as-produced MWCNT(absorbent dose: 1 g/L, pH value: 5.5, C_0: 20 mg/L, contact time: 5, 10, 20, 30, 40, 50, and 60 min, agitation and speed: 200 rpm).

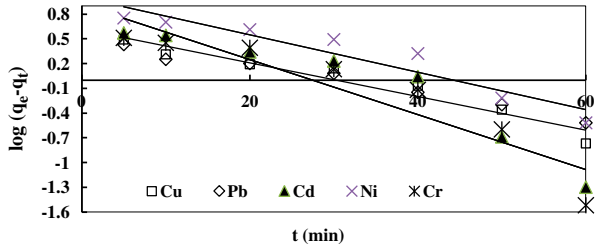

Fig. 10(b). Pseudo-first-order sorption kinetics of metals onto MWCNT-ox (absorbent dose: 1 g/L, pH value: 5.5, C_0: 20 mg/L, contact time: 5, 10, 20, 30, 40, 50, and 60 min, and agitation speed: 200 rpm).

$$\frac{dq}{dt} = \alpha \exp(-\beta q t) \tag{11}$$

To simplify the Elovich equation, Chien and Clayton [35] assumed $\alpha\beta t >> t$, and by applying boundary conditions $q_t = 0 = \text{at } t = 0$ and $q_t = q_t$ and $t = t$, Eq. (11) yields Eq. (12).

$$\frac{dq}{dt} = \frac{1}{B}\ln(\alpha\beta) + \frac{1}{B}\ln(t) \tag{12}$$

where α (mg/g min) is the initial sorption rate and the parameter β (g/mg) is related to the extent of surface coverage and activation energy for chemisorption. The kinetic results will be linear on a q_t vs. ln (t) plot and the constants α and β can be computed from the slope and intercept of the graph.

The kinetic constants obtained from the Elovich equation are listed in Table 3. The correlation coefficients obtained using the Elovich equation were lower than those of the pseudo-second-order equation. So, the Elovich equation might not be sufficient to describe the mechanism and the adsorption process is very fast, probably controlled by chemical adsorption.

3.5. Desorption of metals and reusability of CNTs

The metals mixture loaded MWCNTs were mixed with 10 mL of 5 M HNO_3 for 2 h. The desorption efficiency was found to be 95%. Liang et al. [36] reported that the Cd^{2+}, Mn^{2+}, and Ni^{2+} ions could be effectively desorbed from the MWCNTs by a 1.0 mol/L HNO_3 solution, and the performance was stable up to 50 adsorption–elution cycles. Chen and Wang [37] found that Ni^{2+} desorption was 9% at pH > 5.5, then sharply increased with decreasing pH of the regeneration solution and reached 93% at pH < 2.0.

Table 3
Kinetic parameters for Pb^{2+}, Cu^{2+}, Cr^{6+}, Cd^{2+} and Ni^{2+} adsorption by as produced and oxidized MWCNT (absorbent dose: 1 g/L, pH value: 5.5, initial metals concentration: 20 mg/L, contact time: 5–120 min, and agitation speed: 200 rpm)

	As produced MWCNT					MWCNT-ox				
	Pb^{2+}	Cu^{2+}	Cr^{6+}	Cd^{2+}	Ni^{2+}	Pb^{2+}	Cu^{2+}	Cr^{6+}	Cd^{2+}	Ni^{2+}
Pseudo-first-order	–	–	–	–	–	–	–	–	–	–
q_e (mg/g)(calculated)	3.6	4.8	5.1	3.3	3.2	3.1	4.1	8.2	8.5	10
q_e (mg/g)(experiment)	14	13.4	13	12	11	19.7	19.5	19.25	19.2	19.1
K_1 (min^{-1})	0.03	0.024	0.033	0.01	0.02	0.03	0.04	0.07	0.07	0.05
R^2	0.95	0.91	0.88	0.95	0.88	0.95	0.94	0.9	0.88	0.9
Pseudo-second-order	–	–	–	–	–	–	–	–	–	–
q_e (mg/g) (calculated)	14.3	13.9	13.5	12	11	19.9	19.6	19.6	19.5	19.7
q_e (mg/g)(experiment)	14	13.4	13	12.4	11.3	19.7	19.5	19.25	19.2	19.1
K_2 (g/mg min)	0.02	0.01	0.01	0.01	0.02	0.03	0.02	0.02	0.02	0.01
R^2	0.99	0.99	0.99	0.99	0.99	0.99	0.99	0.99	0.99	0.99
Elovich kinetic model	–	–	–	–	–	–	–	–	–	–
α (mg/g min)	276.4	13261	372.4	1483	3,179	1.68×10^8	7.8×10^6	2.4×10^5	3.3×10^4	4928.3
β (g/mg)	0.78	1.01	0.82	1.04	1.2	1.2	1.04	0.87	0.76	0.68
R^2	0.92	0.95	0.94	0.94	0.92	0.89	0.9	0.9	0.87	0.85

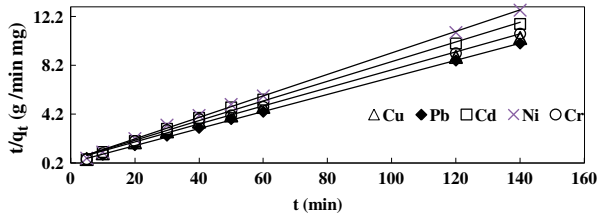

Fig. 11(a). Pseudo-second-order sorption kinetics of metals onto as-produced MWCNT (absorbent dose: 1 g/L, pH value: 5.5, C_0: 20 mg/L, contact time: 5, 10, 20, 30, 40, 50, 60, 90, and 120 min, and agitation speed: 200 rpm).

To study the reusability of CNTs, sorption/desorption process was carried out for metal ions for five cycles. For each cycle, 10 mL of 20 mg/L metals' solution was adsorbed by 20 mg MWCNT-ox for 2 h and then desorbed with 10 mL of 5 M HNO_3 and stirring for 2 h. The sorption capacity was maintained after the cycles of sorption/desorption process.

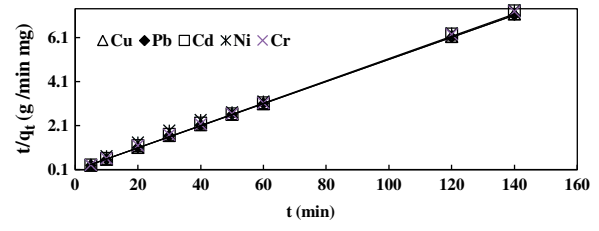

Fig. 11(b). Pseudo-second-order sorption kinetics of metals onto MWCNT-ox (absorbent dose: 1 g/L, pH value: 5.5, initial concentration: 20 mg/L, contact time: 5, 10, 20, 30, 40, 50, 60, 90, and 120 min, and agitation speed: 200 rpm).

4. Conclusions

MWCNTs have been investigated for the removal of copper, lead, cadmium, chromium, and nickel ions from aqueous solutions. The sorption capacities of metal ions to CNTs follow the order: $Pb^{2+} > Cu^{2+} > Cr^{6+} > Cd^{2+} > Ni^{2+}$. Oxidation of MWCNTs with an acid solution improved the sorption capacity of metal ions. Adsorption attained equilibrium at 2 h and was highly dependent on the solution pH and adsorbent dose. The adsorption data were well fitted by both the Langmuir and Freundlich isotherms and the pseudo-second-order kinetics. Sorption/desorption studies showed the possibility to reuse CNTs several times for the sorption of copper, lead, chromium, cadmium, and nickel ions from aqueous solutions.

References

[1] Y.H. Li, S. Wang, J. Wei, X. Zhang, Lead adsorption on carbon nanotubes, Chem. Phys. Lett. 357 (2002) 263.
[2] M.M. Rao, A. Ramesh, G.P.C. Rao, K. Seshaiah, Removal of copper and cadmium from the aqueous solutions by activated carbon derived from ceiba pentandra hulls, J. Hazard. Mater. 129 (2006) 123–129.
[3] M. Sekar, V. Sakthi, S. Rengaraj, Kinetics and equilibrium adsorption study of lead(II) onto activated carbon prepared from coconut shell, J. Colloid Interface Sci. 279 (2004) 307–313.
[4] J. Ayala, F. Blanco, P. García, P. Rodriguez, J. Sancho, Asturian fly ash as a heavy metals removal material, Fuel 77 (1998) 1147–1154.

[5] C.H. Weng, C.P. Huang, Adsorption characteristics of Zn(II) from dilute aqueous solution by fly ash, Colloids Surf., A 247 (2004) 137–143.
[6] Y.S. Ho, G. McKay, The sorption of lead(II) ions on peat, Water Res. 33 (1999) 578–584.
[7] S.C. Pan, C.C. Lin, D. Tseng, Reusing sewage sludge ash as adsorbent for copper removal from wastewater, Resour. Conserv. Recycl. 39 (2003) 79–90.
[8] B. Biskup, B. Subotic, Removal of heavy metal ions from solutions using zeolites. III. Influence of sodium ion concentration in the liquid phase on the kinetics of exchange processes between cadmium ions from solution and sodium ions from zeolite A, Sep. Sci. Technol. 39 (2004) 925–940.
[9] M. Arias, M.T. Barral, J.C. Mejuto, Enhancement of copper and cadmium adsorption on kaolin by the presence of humic acids, Chemosphere 48 (2002) 1081–1088.
[10] C.V. Diniz, F.M. Doyle, V.S.T. Ciminelli, Effect of pH on the adsorption of selected heavy metal ions from concentrated chloride solutions by the chelating resin dowex M-4195, Sep. Sci. Technol. 37 (2002) 3169–3185.
[11] S. Iijima, Helical microtubules of graphitic carbon, Nature 354 (1991) 56–58.
[12] Z.C. Di, J. Ding, X.J. Peng, Y.H. Li, Z.K. Luan, J. Liang, Chromium adsorption by aligned carbon nanotubes supported ceria nanoparticles, Chemosphere 62 (2006) 861–865.
[13] Y.H. Li, Z. Di, J. Ding, D. Wu, Z. Luan, Y. Zhu, Adsorption thermodynamic, kinetic and desorption studies of Pb^{2+} on carbon nanotubes, Water Res. 39 (2005) 605–609.
[14] G.P. Rao, C. Lu, F. Su, Sorption of divalent metal ions from aqueous solution by carbon nanotubes: A review, Sep. Purif. Technol. 58 (2007) 224–231.
[15] Y.H. Li, S. Wang, Z. Luan, J. Ding, C. Xu, D. Wu, Adsorption of cadmium(II) from aqueous solution by surface oxidized carbon nanotubes, Carbon 41 (2003) 1057–1062.
[16] Y.H. Li, J. Ding, Z.K. Luan, Competitive adsorption of Pb , Cu and Cd ions from aqueous solutions by multiwalled carbon nanotubes, Carbon 41 (2003) 2787.
[17] J. Hu, C. Chen, X. Zhu, X. Wang, Removal of chromium from aqueous solution by using oxidized multiwalled carbon nanotubes, J. Hazard. Mater. 162 (2009) 1542–1550.
[18] C.L. Chen, X.K. Wang, Adsorption of Ni(II) from aqueous solution using oxidized multi-walled carbon nanotubes, Ind. Eng. Chem. Res. 45 (2006) 9144–9149.
[19] D. Xu, X. Tan, C. Chen, X. Wang, Removal of Pb (II) from aqueous solution by oxidized multiwalled carbon nanotubes, J. Hazard. Mater. 154 (2008) 407–416.
[20] APHA, Standard Methods for the Examination of Water and Wastewater, 21st ed., American Public Health Association, Washington, DC, 2005.
[21] A. Smara, R. Delimi, E. Chainet, J. Sandeaux, Removal of heavy metals from diluted mixtures by a hybrid ion-exchange/electrodialysis process, Sep. Purif. Technol. 57 (2007) 103–110.
[22] C. Lu, C. Liu, Removal of nickel(II) from aqueous solution by carbon nanotubes, J. Chem. Technol. Biotechnol. 81 (2006) 1932–1940.
[23] N. Nassar, Rapid removal and recovery of Pb(II) from wastewater by magnetic nanoadsorbents, J. Hazard. Mater. 184 (2010) 538–546.
[24] I. Langmuir, The constitution and fundamental properties of solids and liquids. Part I. Solids, J. Am. Chem. Soc. 38 (1916) 2221–2295.
[25] H.M.F. Freundlich, Over the adsorption in solution, J. Phys. Chem. 57 (1906) 385–470.
[26] P. Barkakati, A. Begum, M. Das, Adsorptive separation of Ginsenoside from aqueous solution by polymeric resins: Equilibrium, kinetic and thermodynamic studies, Chem. Eng. J. 161 (2010) 34–45.
[27] C. Kuo, Water purification of removal aqueous copper (II) by as-grown and modified multi-walled carbon nanotubes, Desalination 249 (2009) 781–785.
[28] Ö. Yavuz, Y. Altunkaynak, F. Güzel, Removal of copper, nickel, cobalt and manganese from aqueous solution by kaolinite, Water Res. 37 (2003) 948.
[29] H.K. An, B.Y. Park, D.S. Kim, Crab shell for the removal of heavy metals from aqueous solution, Water Res. 35 (2001) 3551.
[30] N.D. Hutson, R.T. Yang, Theoretical basis for the Dubinin–Radushkevitch (D–R) adsorption isotherm equation, Adsorption 3 (1997) 189–195.
[31] Y.-M. Hao, Chen Man, Z.-B. Hu, Effective removal of Cu (II) ions from aqueous solution by amino-functionalized magnetic nanoparticles, J. Hazard. Mater. 184 (2010) 392–399.
[32] Y.S. Ho, Citation review of Lagergren kinetic rate equation on adsorption reactions, Scientometrics 59 (2004) 171–177.
[33] Y.S. Ho, Review of second-order models for adsorption systems, J. Hazard. Mater. 136 (2006) 681–689.
[34] D.L. Sparks, Kinetics of Reaction in Pure and Mixed Systems in Soil Physical Chemistry, CRC Press, Boca Raton, 1986, pp. 12–18.
[35] S.H. Chien, W.R. Clayton, Application of Elovich equation to the kinetics of phosphate release and sorption in soils1, Soil Sci. Soc. Am. J. 44 (1980) 265–268.
[36] P. Liang, Y. Liu, L. Guo, J. Zeng, H. Lu, Multiwalled carbon nanotubes as solid-phase extraction adsorbent for the preconcentration of trace metal ions and their determination by inductively coupled plasma atomic emission spectrometry, J. Anal. At. Spectrom. 19 (2004) 1489–1492.
[37] C. Chen, X. Wang, Adsorption of Ni(II) from aqueous solution using oxidized multiwall carbon nanotubes, Ind. Eng. Chem. Res. 45 (2006) 9144–9149.